Role of Long Range Interaction in Oxygen Superstructure Formation on Cu(001) and Ni(001)

Sergey Stolbov and Talat S. Rahman

Department of Physics, Cardwell Hall, Kansas State University, Manhattan, Kansas 66506

(Received 31 May 2002; published 23 August 2002)

On the basis of electronic structure calculations, we show that the long range Coulomb interaction provides the driving mechanism for oxygen overlayer formation on Cu(001). We illustrate that this interaction in the precursor $c(2 \times 2)$ phase induces a missing row reconstruction of Cu(001), and leads to the $(2\sqrt{2} \times \sqrt{2})R45°$ O structure, which has strong covalent pO–dCu coupling. For the $c(2 \times 2)$O overlayer on Ni(001) and Cu(001), we show that pO–dNi bonding is larger than pO–dCu and serves to neutralize the perturbation of the Coulomb interaction induced by the O overlayer. Consequently, $c(2 \times 2)$O/Ni(001)) is stable while $c(2 \times 2)$O/Cu(001) exists only in limited environments.

DOI: 10.1103/PhysRevLett.89.116101 PACS numbers: 68.43.–h, 71.15.Ap, 73.20.Hb

The chemisorption of oxygen on metal surfaces attracts attention of many researchers, because it is related to technologically important processes, such as corrosion and catalysis. Furthermore, an understanding of the nature of this phenomenon is expected to serve as a prototype for the fundamental knowledge of the interaction between gases and solid surfaces. Over the years, oxygen adsorbates on Ni(001) and Cu(001) surfaces have served as excellent model systems for studying the chemisorption process, because, on the one hand, they are apparently similar (both Ni and Cu are fcc metals and neighbors in the periodic table), and, on the other, they demonstrate very different structural behavior. It is now well accepted that on Ni(001) a simple $c(2 \times 2)$ phase is formed for 0.5 ML (monolayer) in which the O atoms occupy fourfold hollow sites at a distance of about 0.8 Å above the Ni surface [1,2]. In the case of O/Cu(001) with a similar coverage, a much more complicated superstructure is formed which has the periodicity $(2\sqrt{2} \times \sqrt{2})R45°$ [3] and involves missing rows of Cu atoms [4,5]. Both structures are schematically illustrated in Fig. 1. This dramatic difference in atomic structures raises questions about its driving forces, which are expected to be related to the idiosyncrasies of their electronic structure. Earlier theoretical studies, based on simple electronic structure models, have correlated the structural properties of the O/Cu(001) system to a strong pO–dCu hybridization [6] and charge transfer [7] in the vicinity of the surface. Calculations using more realistic techniques [8,9] for $c(2 \times 2)$ O/Cu(001) confirm that the hybridization and charge transfer are noticeable, but they make no attempt to examine their role in formation of the $(2\sqrt{2} \times \sqrt{2})R45°$ phase.

To evaluate the factors potentially responsible for superstructure formation on Cu(001), consider the observed systematics of O deposition on Cu(001). According to experimental results summarized in Refs. [10,11], at a low coverage, oxygen forms $c(2 \times 2)$ islands and, only when the coverage exceeds 0.34 ML, the system undergoes the missing row reconstruction and the $(2\sqrt{2} \times \sqrt{2})R45°$ phase is formed [3]. This suggests that O atoms may interact locally with Cu(001) and Ni(001) in similar manners and, only beyond certain coverage, some other factor(s) may play a dominant role in determining the surface structure. What could this factor be? The hybridization of the O and metal electronic states is a local effect which cannot depend explicitly on coverage, but the O–O bonding could be coverage dependent. However, in $c(2 \times 2)$ O/Cu(001), the shortest O–O distance is too long (more than 5 Å) to provide a noticeable pO–pO hybridization. In this Letter, we show that the long range Coulomb

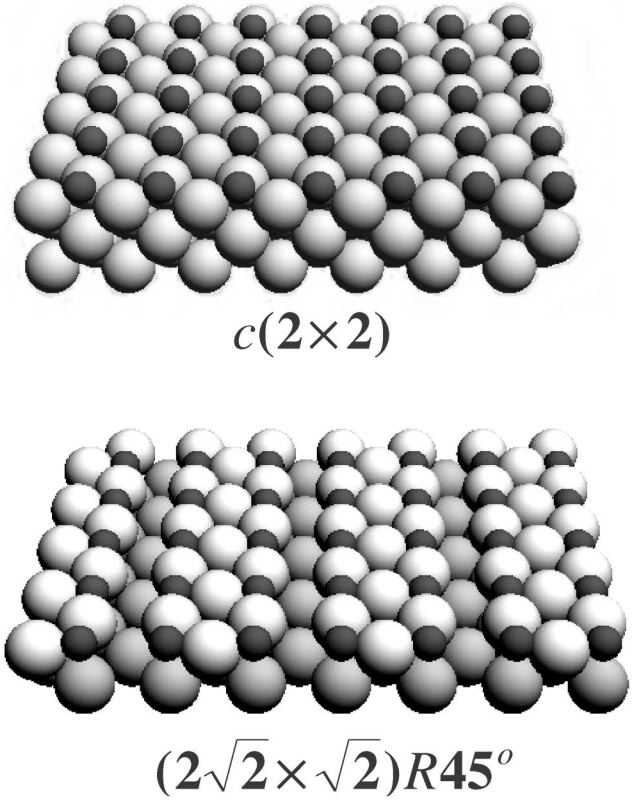

FIG. 1. Schematic illustration of the $c(2 \times 2)$ and $(2\sqrt{2} \times \sqrt{2})R45°$ structures of O/M(001), where M denotes an fcc metal.

interaction between the O overlayer and the metal surface is the driving force for the instability of the $c(2 \times 2)$ O superstructure on Cu(001) and leads to the subsequent reconstruction of the substrate. We provide an estimate of the magnitude of this effect by calculating the Madelung potentials at different sites, for a set of observed and hypothetical structures of O on Cu(001). Keeping in mind that any equilibrium structure is formed as a result of competition between several effects, we also analyze the elements of covalent binding and charge transfer in the systems, using first principles electronic structure calculations. Finally, we extend the calculations to the case of the $c(2 \times 2)$ O overlayer on Ni(001) to identify the cause for the difference with the O/Cu(001) system.

We calculate the surface Madelung potentials within muffin-tin (MT) approximation using the technique developed in Ref. [12] in which the space in the vicinity of the surface is divided into layers belonging to different atomic planes parallel to the surface. The interstitial charge density ρ_i^0 is supposed to be layer dependent, reflecting the asymmetry of the system (i denotes the layer number). The Madelung potential includes the MT monopole $M_{i\alpha,j\beta}^{00}$ and interstitial $V_{ij}[\rho_j]$ terms [12]:

$$V_{i\alpha}^{\mathrm{Mad}} = \sum_{j,\beta} (q_{j\beta} M_{i\alpha,j\beta}^{00} + V_{ij}[\rho_j]), \tag{1}$$

where

$$q_{j\beta} = Z_{j\beta} - q_{j\beta}^{\mathrm{MT}} + \rho_j \omega_{j\beta}, \tag{2}$$

α and β label atoms belonging to the ith layer, $Z_{j\beta}$ are atomic numbers, and $q_{j\beta}^{\mathrm{MT}}$ denote electronic charges within MT spheres of volume $\omega_{j\beta}$.

To get a simple and intuitive picture, we first calculate the Madelung potential for several surface structures within a "frozen" charge density approximation using Eq. (1). Namely, we calculate the effective charges $q_{i\alpha}$ introduced in Eq. (2) using bulklike electronic density for Cu and atomlike density for O. As expected, the presence of the surface itself causes only a small perturbation in the Madelung potential (see the column under "clean" in Table I). The $c(2 \times 2)$ superstructure on Cu(001), for which we have taken the surface structural parameters from Ref. [11], causes a very large perturbation in the Madelung potential in the top Cu layer, as seen in Table I. The missing row reconstruction understandably makes some Cu sites nonequivalent in the structure. In Fig. 2, these nonequivalent atoms are shown and labeled for further discussions. Turning to Table I, the missing Cu rows themselves are found to reduce considerably the perturbation of the Madelung potential in the top Cu layer, and slightly increase it in some of the lower Cu sites (column MR in Table I). Further reconstruction and relaxation leading to the stable $(2\sqrt{2} \times \sqrt{2})R45°$ O/Cu(001) structure indeed result in a significant reduction of the perturbation from the values of $c(2 \times 2)$ and MR configurations, for all atomic sites (column MRRR in Table I).

TABLE I. The variation of the Madelung potential (in Ry) at different atomic sites with respect to the bulk value for the following configurations: clean Cu(001) (Clean); $c(2 \times 2)$ O on Cu(001) [$c(2 \times 2)$]; $(2\sqrt{2} \times \sqrt{2})R45°$ O on bulk terminated O/Cu(001) with missing rows (MR); $(2\sqrt{2} \times \sqrt{2})R45°$ O/Cu(001) relaxed and reconstructed (MRRR).

Layer	Site	Clean	$c(2 \times 2)$	MR	MRRR
	O	⋯	−0.329	−0.379	−0.880
I	Cu1	−0.007	1.810	0.495	0.219
	Cu2	−0.007	1.810	1.022	0.660
	Cu3	0.002	−0.113	−0.207	0.008
II	Cu4	0.002	−0.113	0.271	0.299
	Cu5	0.002	−0.113	0.478	0.162
III	Cu6	0.001	0.010	0.016	0.011
	Cu7	0.001	0.010	0.100	0.037
IV	Cu8	0.0	0.0	0.003	0.0
V	Cu9	0.0	0.0	0.0	0.0

Such a clear correlation between the strength of the perturbation of Madelung potential and system geometry suggests that the long range Coulomb interaction is a driving force for the missing row reconstruction in O/Cu(001). This is, however, just an initial factor controlling properties of the system which is expected to be followed by charge transfer and modification of chemical bonds. Since these effects can be properly analyzed only through reliable self-consistent electronic structure calculations, we have carried out such calculations for the three systems in question: $c(2 \times 2)$ O/Cu(001), $(2\sqrt{2} \times \sqrt{2})R45°$ O/Cu(001), and $c(2 \times 2)$ O/Ni(001), using the locally self-consistent multiple scattering (LSMS) method in the real space representation for the Green's function [13]. The effect of the surface on the MT potential is taken into account using the approach developed in Ref. [12]. Within the LSMS method, calculations of the Green's function are performed for a set of overlapping clusters centered on the nonequivalent atomic sites. We used nine

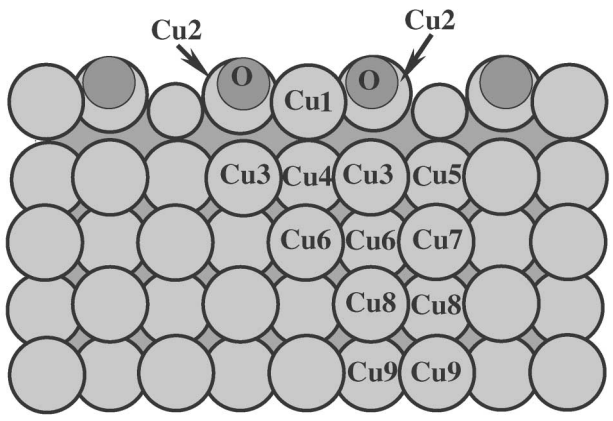

FIG. 2. Side view of $(2\sqrt{2} \times \sqrt{2})R45°$ O/Cu(001) with numbered nonequivalent atoms.

clusters containing 62 to 91 atoms for $(2\sqrt{2} \times \sqrt{2})R45°$ and five clusters of 71 to 79 atoms for $c(2 \times 2)$ systems. More details of the calculations can be found elsewhere [14,15].

For all three systems, we find a significant valence electronic charge redistribution as a response to the perturbation of the potential described above. The oxygen charge variation ΔQ_O, which is the difference between the charge on oxygen in the system and in the atomic state, is calculated by integrating the self-consistent valence charge density over spheres centered at the O sites. For uniformity, spheres with a fixed radius of 0.935 Å (one-half of the shortest O–M bond length) are used for all three systems. For $(2\sqrt{2} \times \sqrt{2})R45°$ O/Cu(001) and $c(2 \times 2)$ O/Ni(001), ΔQ_O is found to be $0.642e$ and $0.848e$, respectively, reflecting electronic charge transfer from the metal surfaces to O. For the elusive $c(2 \times 2)$ O/Cu(001) structure, at O–Cu spacing close to the experimental value (0.72 Å) [11], a much larger value $\Delta Q_O = 1.043e$ is found. The comparatively stronger perturbation of the local potentials in $c(2 \times 2)$ O/Cu(001) is thus seen to cause a larger increase in the valence electronic charge density at the O sites that may result in an enhancement of electron-electron repulsion and, hence, contribute to an increase in the energy of the system.

Because the screening of the perturbation in the systems is partial, the energetics of the self-consistent local potentials are found to be different for nonequivalent Cu sites in both O/Cu(001) systems. It can be characterized quantitatively by shifts of the single-site d-resonance energy with respect to its bulk value. For $(2\sqrt{2} \times \sqrt{2})R45°$O/Cu(001), these shifts are found to be $+0.065$ Ry, -0.099 Ry, $+0.109$ Ry, and $+0.134$ Ry for the Cu2, Cu3, Cu4, and Cu5 sites, respectively [for comparison, for the first layer of clean Cu(001) this shift is equal to -0.009 Ry]. These shifts cause a differential energetic separation of pO and dCu subbands for nonequivalent Cu atoms, leading to a hierarchy of covalent pO–dCu binding: the higher the separation, the weaker the binding. As a result, the covalent pO–dCu3 coupling in $(2\sqrt{2} \times \sqrt{2})R45°$ O/Cu(001) is found to be stronger than the coupling between O and its other nearest neighbors (Cu1, Cu2), though the O–Cu3 bond length is longer than either O–Cu1 or O–Cu2 [15]. Thus, the long range Coulomb interaction implicitly influences short range effects such as covalent binding.

An analysis of the calculated densities of electronic states for the three systems shows that, in $(2\sqrt{2} \times \sqrt{2})R45°$ geometry, the O–p_z and Cu3–d_{3z^2-1} states are more involved in hybridization than the others [15], whereas in the $c(2 \times 2)$ geometry it is the O–p_x and M–d_{xz} states (M = Cu, Ni) [14]. As shown in Fig. 3, O–p_z and Cu3–d_{3z^2-1} states in $(2\sqrt{2} \times \sqrt{2})R45°$ O/Cu(001) display a nice splitting. They form a common subband represented by peaks "a" and "b," which are separated by about 0.57 Ry. This strong splitting together with the involvement of a major part of these states in hybridization (redistributed into "a" and "b" regions) are clear signatures of strong covalent binding. In the case of $c(2 \times 2)$ O/Cu(001), the corresponding splitting in Fig. 3 is much smaller. Further, unlike the $(2\sqrt{2} \times \sqrt{2})R45°$ structure, the antibonding peak "b" in $c(2 \times 2)$ O/Cu(001) is completely occupied, signifying a weaker covalent pO–dCu binding, as already suggested [6].

As seen in Fig. 3, the energetic separation between the peak "a" in the bonding O–p_x substructure and antibonding peak "b" are 0.37 Ry and 0.46 Ry for O/Cu(001) and O/Ni(001), respectively. Thus, for almost the same d_{O-M} [0.72 Å for O/Cu(001) and 0.7 Å for O/Ni(001)], the splitting is found to be 24% higher for O/Ni(001) than for O/Cu(001). Furthermore, the antibonding peak is completely occupied in O/Cu(001), whereas it is pinned at the Fermi level in O/Ni(001). These findings also indicate that the covalent pO–dM binding is much stronger in O/Ni(001) than in O/Cu(001). Of course, this conclusion is reflective of the fact that the valence d wave function is more extended in Ni than in Cu which allows larger spatial overlap, and stronger covalent bonding, for almost the

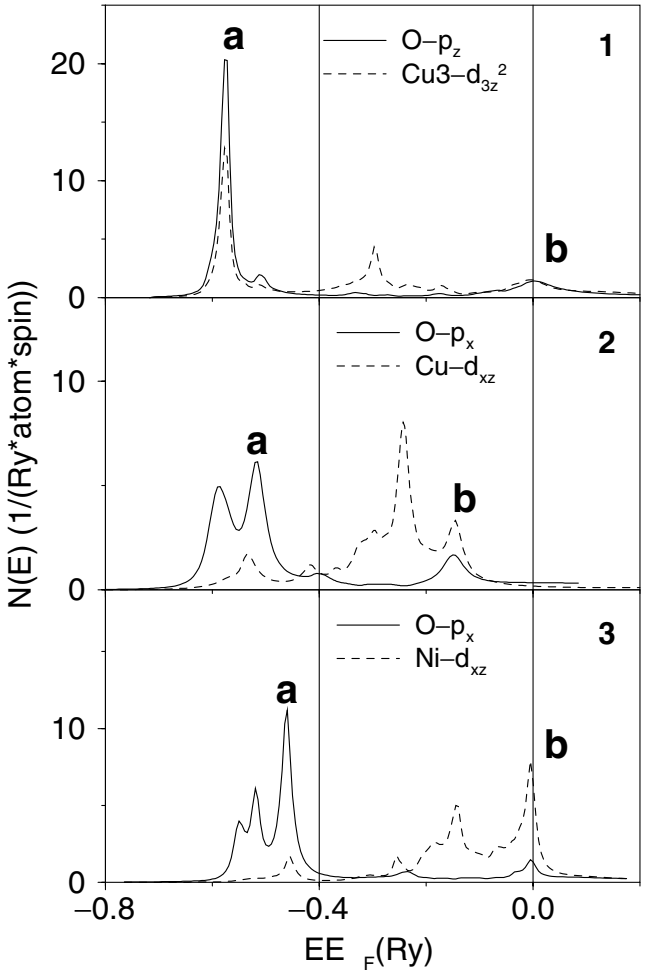

FIG. 3. Projections of the densities of pO- and dM-electronic states (M = Cu, Ni) which form covalent bonds in $(2\sqrt{2} \times \sqrt{2})R45°$ O/Cu(001) (panel 1), in $c(2 \times 2)$ O/Cu(001) (panel 2), and in $c(2 \times 2)$ O/Ni(001) (panel 3).

same O–metal bond length, for the pO–dNi states, than for the pO–dCu states.

The above analysis leads to the following picture for oxygen adsorption on Ni(001) and Cu(001). As the O overlayer approaches the metal surface, it produces the following: (i) an increase in the long range Coulomb interaction which pulls up the local potentials at the top (metal) layer sites and induces an electronic charge transfer from the host surface to the O atoms; (ii) an enhancement of the covalent pO–dM binding. The first effect tends to increase the total energy of the system while the second reduces it. Relative magnitudes of these two effects are different in O/Cu(001) and O/Ni(001). Since the Ni d-wave function is more extended than that of Cu, the covalent pO–dM binding is stronger in O/Ni(001) than in O/Cu(001). In addition, the charge transfer is smaller in O/Ni(001) than in O/Cu(001).

In O/Ni(001), the competition of the two effects results in a minimum in total energy for a specific value of $d_{\mathrm{O–Ni}}$ making the $c(2 \times 2)$ structure stable, whereas in O/Cu(001) such a minimum does not appear for 0.5 ML because of comparative weakness of the covalent bonds and strength of the Coulomb repulsion. At lower O coverages (say, 0.34 ML), the long range interaction is weaker and it may be balanced by the covalent bonding. It is thus not surprising that small islands of $c(2 \times 2)$ O/Cu(001) are observed in a number of experiments and not in well ordered large domains. Moreover, missing row reconstruction and further lattice relaxation dramatically reduce the long range Coulomb interaction and strengthen the covalent pO–dCu bonds that stabilize the $(2\sqrt{2} \times \sqrt{2})R45°$ O/Cu(001).

In summary, we have shown here that the long range Coulomb interaction plays a critical role in determining the geometry of the oxygen overlayer on Cu(001). While local effects such as charge transfer and hybridization have been proposed as possible rationale for the instability of the $c(2 \times 2)$ O overlayer on Cu(001) [versus that on Ni(001)], to our knowledge, neither a quantification of these local effects nor the presentation of a consistent picture which connects the short and long range behavior of these system has yet been done. Our conclusions provide a sound basis for understanding both the presence of the $c(2 \times 2)$ O/Cu(001) structure in the form of small islands (because the perturbation in the Madelung potential is not as strong for them) and stability of the $(2\sqrt{2} \times \sqrt{2})R45°$ O superstructure on Cu(001) at 0.5 ML coverage. Furthermore, the same arguments attest to the relative stability of the $c(2 \times 2)$ overlayer on Ni(001) as compared to that on Cu(001). Finally, the approach presented here has more general applicability to other light gas adsorbates on metal surfaces. Indeed, moving from O to the left in the periodic table (to N and C), the effective radius of the valence p wave function increases. Consequently, we expect that at a specific adsorbate–top metal spacing, the adsorbate–metal covalent binding is enhanced when moving from O to N and from N to C. On the other hand, the more extended the valence wave functions, the larger the effective charges $q_{j\beta}$ in Eq. (2) and, hence, the larger the contribution of the adsorbent to the Madelung potential. We thus expect that the competition between the long range Coulomb interaction and covalent coupling to be important for overlayer formation of C and N on Ni and Cu surfaces. Furthermore, the effects described here are expected to play an even larger role on stepped surfaces on which oxygen has been found to produce faceting and step doubling [16,17]. We leave these studies for the future.

This work was supported in part by NSF under Grant No. CHE-0205064. We thank A. Kara for many helpful discussions. T. S. R. also thanks the Alexander von Humboldt Foundation for a Forschungspreiz and thanks her hosts at the Fritz Haber Institute in Berlin for hospitality.

[1] K. Heinz, W. Oed, and J. B. Pendry, Phys. Rev. B **41**, 10 179 (1990).
[2] W. Oed, H. Lindner, U. Starke, K. Heinz, and K. Müller, Surf. Sci. **224**, 179 (1989).
[3] M. Wuttig, R. Franchy, and H. Ibach, Surf. Sci. **213**, 103 (1989).
[4] A. Atrie, U. Bardi, G. Casalone, G. Rovida, and E. Zanazzi, Vacuum **41**, 333 (1990).
[5] I. K. Robinson, E. Vlieg, and S. Ferrer, Phys. Rev. B **42**, 6954 (1990).
[6] K. W. Jacobsen and J. K. Norskov, Phys. Rev. Lett. **65**, 1788 (1990).
[7] E. A. Colbourn and J. E. Inglesfield, Phys. Rev. Lett. **66**, 2006 (1991).
[8] P. V. Madhavan and M. D. Newton, Chem. Phys. **86**, 4030 (1987).
[9] T. Wiell, J. E. Klepeis, P. Bennich, O. Björneholm, N. Wassdahl, and A. Nilsson, Phys. Rev. B **58**, 1655 (1998).
[10] T. Fujita, Y. Okawa, Y. Matsumoto, and K. I. Tanaka, Phys. Rev. B **54**, 2167 (1996).
[11] M. Kittel, M. Polcik, R. Terborg, J.-T. Hoeft, P. Baumgärtel, A. M. Bradshaw, R. L. Toomes, J.-H. Kang, D. P. Woodruff, M. Pascal, C. L. A. Lamont, and E. Rotenberg, Surf. Sci. **470**, 311 (2001), and references therein.
[12] L. Szunyogh, B. Ujfalussy, P. Weinberger, and J. Kollar, Phys. Rev. B **49**, 2721 (1994).
[13] Y. Wang, G. M. Stocks, W. A. Shelton, D. M. C. Nicholson, Z. Szotek, and W. M. Temmerman, Phys. Rev. Lett. **75**, 2867 (1995).
[14] S. Stolbov, A. Kara, and T. S. Rahman (to be published); cond-mat/0111145, 2001.
[15] S. Stolbov and T. S. Rahman (to be published); cond-mat/0203277, 2002.
[16] S. Vollmer, A. Birkner, S. Lucas, G. Witte, and Ch. Wöll, Appl. Phys. Lett. **76**, 2686 (2000).
[17] A.-M. Lanzillotto and S. L. Bernasek, Surf. Sci. **175**, 45 (1986).